Effect of the Formation of Inclusion Complexes With β-Cyclodextrin on the Photoisomerization and Fluorescence Properties of Aromatic Norbornadiene Derivatives

MOUNIR MAAFI, JEAN-JACQUES AARON* and CLAUDE LION
Institut de Topologie et de Dynamique des Systèmes de l'Université de Paris 7 Denis Diderot, associé au CNRS, URA 34, 1, rue Guy de la Brosse, 75005 Paris, France.

Abstract. The valence photoisomerization of four aromatic norbornadiene (NBD) derivatives has been studied in ethanol and in 0.01 M β-cyclodextrin (β-CD) water–ethanol (v/v, 99/1) solution (WECD). Observed first-order rate constants are found to be of the same order of magnitude in ethanol and WECD, ranging between 0.1 and 0.28 s^{-1}, according to the compound. These photoisomerization kinetic properties are attributed to the formation of inclusion complexes between NBDs and β-CD. The stoichiometry is 1:1, and association constants ranging between 310 and 390 M^{-1} have been determined fluorimetrically, using Benesi–Hildebrand plots and a nonlinear regression method. The structure of the inclusion complexes is discussed on the basis of AMI semiempirical dimension calculations and photophysical properties.

Key words: Norbornadiene, β-cyclodextrin, inclusion complex, photoisomerization, fluorescence, absorption spectrophotometry.

1. Introduction

Cyclodextrins (CDs) are toroidal, hollow-shaped, cyclic oligosaccharides connected by $\alpha(1$–$4)$ linkages. The three major, well-known, and industrially produced CDs are composed of 6, 7 or 8 glucose units, called α-, β- and γ-cyclodextrin, respectively. Because of their enhanced hydrophilic capacity due to the presence of primary and secondary hydroxyl groups on the CD exterior molecular surface, they are hydrosoluble. In contrast, the aligned glycosidic oxygens and C—H groups located in the inner cavity wall make the interior of the CD hydrophobic. For these reasons, CDs have the ability to extract from aqueous media and to accommodate in their cavity a variety of organic molecules. This inclusion ability is the most important property of CDs. Thereby, the partial or total binding of the guest molecule into the CD (host) cavity leads to the formation of inclusion complexes. Complexation is governed by various types of interactions, including geometrical
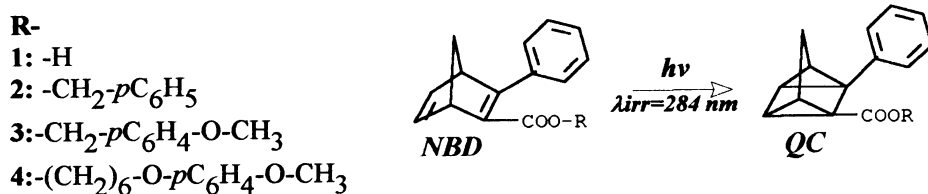
---
* Author for correspondence.

steric factors, hydrophobic interactions, hydrogen bonding, and London dispersion forces [1, 2].

Generally, such supramolecular and hydrosoluble systems produce important changes of the photophysical and/or photochemical properties of the included guests. Fluorescence [3], room-temperature phosphorescence [4], and circular dichroism signals [5], are increased or induced for several organic compounds in the presence of CD, in aqueous solutions.

Moreover, CD inclusion complexes alter the behaviour of many photoreactions in aqueous media [6–26]. For instance, the photostability of several photosensitive drugs is enhanced in the presence of CDs [1, 3–6]. The photooxidation of Azure A is retarded on formation of a binary inclusion complex with β-CD [6], whereas, the photodimerization of hydrosoluble anthracene derivatives is greatly accelerated by γ-CD [7]. Also, the product distribution of the photo-Fries rearrangement of esters and amides changes significantly in the presence of γ-CD [8]. Flamigni [9] has established that the photoreactivity of triplet and radical intermediates of rose bengal and erythrosin B was slower in complexes with α- and γ-cyclodextrins than in water.

Several photoisomerization reactions of CD-encapsulated compounds have been recently studied [17–26]. For instance, Inoue *et al.* [17] reported the inclusion-enhanced optical yield and E/Z ratio photoisomerization of cyclooctene in the presence of β-cyclodextrin monobenzoate derivative. In contrast, inclusion in α- and β-CD provokes a deceleration of both photoisomerization and photodimerization kinetics of translat [18]. Fukushima *et al.* [19] investigated the photochemical properties of a pendant and photoresponsive azobenzene covalently linked to β-CD. Bortolus *et al.* [20] showed that the quantum yields of the *trans* $\rightleftharpoons$ *cis* azobenzene photoisomerization are strongly reduced in the presence of complexing α-, β- and γ-cyclodextrins, with respect to aqueous medium.

An interesting photoreactive model compound is constituted by norbornadiene (NBD). In fact, NBD and its derivatives are easily photoisomerized into quadricyclanes (QC) upon UV irradiation [27, 28]. Back reversion of the latter molecules to initial NBDs, releasing the stored energy thermally, is generally carried out in the presence of an adequate catalyst [29]. Since this cyclic process can be repeated a number of times, the NBD : QC system has received a great deal of attention either for use as a photoswitching device or for photochemical light storage and solar energy conversion [30]. Also, chemically [31] or electrochemically synthesized polymers [32], bearing NBD pendant rings, have been recently tested as new materials for the storage of sunlight. NBD photoisomerization has been widely investigated in organic solvents [27–32] but very seldom in aqueous media [33], partly because NBD derivatives are generally not hydrosoluble. Until now, only one study has been reported on the photosensitized photochemical reactivity of some low-UV absorbing, and bridge-substituted NBD derivatives in the presence of β-CD [34].

R-
1: -H
2: $-CH_2\text{-}pC_6H_5$
3: $-CH_2\text{-}pC_6H_4\text{-}O\text{-}CH_3$
4: $-(CH_2)_6\text{-}O\text{-}pC_6H_4\text{-}O\text{-}CH_3$

Scheme 1. Structure of the aromatic NBD derivatives and their QC isomers (**1–4**).

The aim of this work is to investigate the formation of β-CD inclusion complexes with four new aromatic NBD derivatives (see structures in Scheme 1). As shown in a preliminary communication [35], complexation should increase the NBDs solubility in aqueous medium and make it possible to measure the photoisomerization kinetics of these hydrophobic NBD molecules in water.

Moreover, we have studied the effect of β-cyclodextrin on the electronic spectral properties of these aromatic NBDs in aqueous media, and we have determined spectrofluorimetrically the stoichiometry and formation constants of the NBDs : β-CD inclusion complexes.

2. Experimental

2.1. REAGENTS

The chemical syntheses of the four NBD derivatives under study have been described elsewhere [28]. A Diels–Alder reaction and a phase transfer catalysis method were applied. β-Cyclodextrin was obtained from Janssen Chemica (analytical grade) and used as received. Distilled water and ethanol (Merck) were used throughout.

2.2. INSTRUMENTATION AND EXPERIMENTAL CONDITIONS

Absorption and fluorescence excitation and emission spectra were recorded at room temperature (298 K) on a Varian DMS 200 spectrophotometer and a Perkin Elmer Model LS-5 luminescence spectrometer, respectively. Fluorescence data acquisition and data analysis were performed by using a software program written in our laboratory. The instrument working conditions were: excitation and emission bandwidth 5 nm and scan rate of spectral acquisition 120 nm/min. All measurements were performed in a 1-cm quartz cuvette.

2.3. PHOTOIRRADIATION CONDITIONS

An Osram 200 W high-pressure mercury lamp with an Oriel Model 8000 power supply, placed in a Schoeffel instrument GMBH type 102 housing, was used for sample irradiation. The output excitation light wavelength was centered around

284 nm, using a 37-nm bandwidth interference filter. The photolysis quartz cell was placed at a distance of 30 cm from the lamp and the solution was stirred magnetically during irradiation.

2.4. PROCEDURE AND SAMPLE PREPARATION

Because of the low solubility of NBD derivatives in water, 5×10^{-3} M stock solutions were prepared in ethanol. 5×10^{-5} M aqueous solutions were obtained by serial dilutions in a total volume of 10 mL containing 0.1 mL of NBD ethanolic solution, and making up to the mark with distilled water. Under these conditions, all NBD solutions are apparently homogeneous. An aliquot of the NBD working solution was irradiated with UV filtered-light of the mercury lamp at suitable time intervals.

For β-CD concentration studies, the solutions were prepared by adding in a 10-mL precision flask, first, a 0.1-mL NBD ethanolic stock solution, then a varying volume of a 10^{-2} M stock β-CD aqueous solution and making up to the mark with distilled water. The formation constants of the complexes were determined by a nonlinear regression (NLR) method, using an Origin, version 2.1, iterative software program.

The kinetic measurements were performed on 5×10^{-5} M NBD solutions containing 10^{-2} M β-CD, and irradiated under standard conditions. The samples were analysed successively by fluorescence and absorption spectrometry. The absorption and fluorescence emission spectral data were treated by the Guggenheim method using linear least-squares regression, to determine the observed first-order rate constants (k_{obs}) [28,36]. This method allows the evaluation of the rate constants without determining experimental values at the limit conditions, as previously discussed [28].

3. Results and Discussion

The absorption and fluorescence excitation and emission characteristics of the NBD derivatives were investigated at room temperature in ethanol (EtOH) and in 0.01 M β-CD water–ethanol mixture (v/v, 99/1) (WECD).

3.1. ELECTRONIC ABSORPTION SPECTRA OF NBD SOLUTIONS

Figure 1 shows typical absorption spectra of 5×10^{-5} M NBD derivatives, obtained in EtOH and WECD. As can be seen in Table I, the absorption spectra recorded in both media exhibit generally, three maxima, located in the 200–210 nm, 220–225 nm and 285–290 nm regions. The first two bands, with high molar absorption coefficients (log ϵ = 4.1–4.6) can be attributed to a combination of the aromatic ^1B transition and the norbornadiene intramolecular charge transfer transition [28, 37]. The long wavelength transition band ($\lambda \cong 290$ nm), with smaller molar absorption coefficients, corresponds to the benzene ^1L_a and ^1L_b transitions (π, π^*) [28].
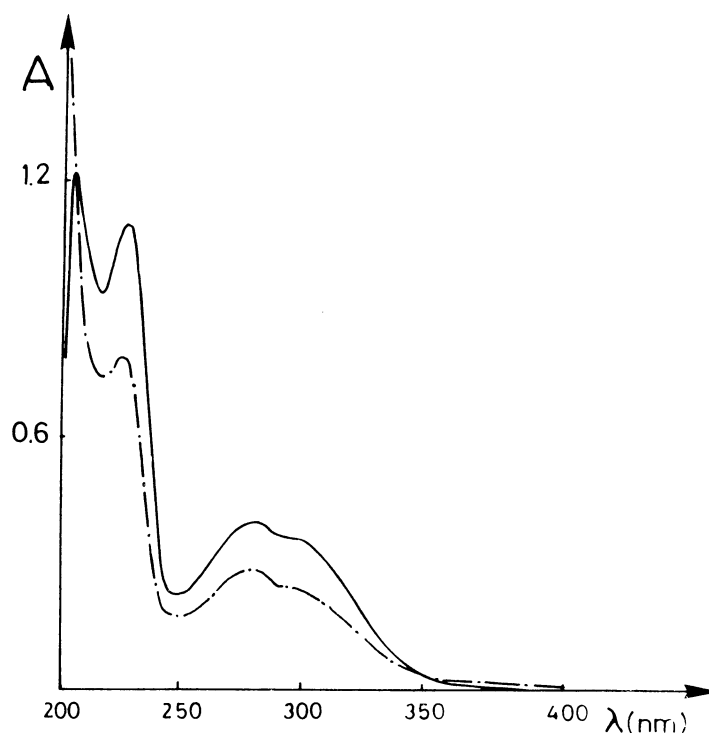
Figure 1. Electronic absorption spectra of compound **3** (5×10^{-5} M) in ethanol (———), and in a 10^{-2} M β-CD 99 : 1 water–ethanol (–•–).

Table I. Absorption spectral characteristics of NBD derivatives in the different media.[a]

Compound	$\lambda_{abs}(\log \epsilon)$[b] in:	
	Ethanol	Water/Ethanol/β-CD
1	288(3.85), 205(4.55)	285(3.85), 225(4.13)
2	293(3.74), 205(4.35)	292(3.84), 227(4.03)
3	298(3.84), *276*(3.95),	*294*(3.68), 277(3 .74),
	224(4.33), 203(4.39)	224(4.19)
4	290(3.40), 224(3.79),	287(3.88), 231(4.24)
	203(4.11)	

[a] 5×10^{-5} M concentration in all cases.
[b] λ_{abs} absorption wavelength maxima (underlined) and shoulders (in italics). ϵ = molar absorption coefficients (M^{-1} cm^{-1}).

In contrast, in water-ethanol (v/v, 99/1) (WE), the absorption spectra are very poorly resolved and no very-well defined peak, but a very wide band, can be distinguished in the 200–360 nm region. This may be attributed to aggregate for-

mation, strong solvation, microheterogeneity effects, and/or homogeneous dispersion occurring in this predominantly aqueous medium in which the NBD aromatic derivatives are slightly soluble.

Although similar spectral characteristics are observed in EtOH and WECD for all NBD derivatives, a decrease of the molar absorption coefficient, more pronounced for the short than for the long wavelength bands, is noted in the latter medium relative to the former. In addition, the long wavelength absorption band maximum is practically unshifted, while the short wavelength band maximum seems to be shifted to wavelengths below 200 nm. Analogous small spectral changes have been reported for a variety of organic compounds in β-CD aqueous solutions [1].

The comparison of the spectral properties in these media suggests that specific interactions take place between the NBD aromatic derivatives and β-CD molecules in the WECD medium.

3.2. Medium effect on the aromatic NBDs fluorescence characteristics

We have found previously [28], that, except for compound **1**, the NBD aromatic derivatives under study are fluorescent. Generally, the fluorescence excitation spectra in organic solvents (including ethanol), consist of two bands located close to the absorption maxima. The fluorescence emission maximum of derivatives **2**–**4** occurs in the 300–350 nm region. This band has been attributed to the π^*, π deactivation transitions belonging to the phenylester groups of these compounds.

The fluorescence excitation peak maxima recorded in EtOH are not shifted relative to those obtained in WECD, for compounds **2** and **3** (Table II). In contrast, for compound **4**, a small blue shift ($\Delta\lambda = 13$ nm) is observed in WECD relative to EtOH. In the case of emission spectra, weak red shifts ($\Delta\lambda = 2$–8 nm) are noted upon changing the medium from EtOH to WECD (Figure 2 and Table II). In contrast, the spectrum obtained in WE shows a broad fluorescence emission band between 330 nm and 450 nm, which may be explained by the same reasons as those given for the absorption spectra in WE.

In contrast with absorption spectral results, significant changes of the relative fluorescence intensity (F) occur according to the medium. Indeed, depending on the compound, the fluorescence intensity is about 1.6 to 3 times higher in WECD, than in ethanol (Figure 2 and Table II).

Such fluorescence intensity enhancements taking place in the presence of β-CD have been extensively discussed by several authors [1–3, 5b, 6]. This behaviour is attributed to the formation of an inclusion complex between the organic compound (here, the NBD derivative) and cyclodextrin (CD). Indeed, the literature data suggest that inclusion in CD does not considerably disturb the ground and excited singlet state energy levels. But inclusion plays an important role in decreasing the rate of nonradiative deactivating process of the singlet or triplet states [5a]. This probably

Table II. Fluorescence spectral properties and β-CD equilibrium formation constants (K_1, in M^{-1}) of NBD derivatives.[a]

Compound	Medium	λ_{exc}, (nm)[b]	λ_{em}, (nm)[b]	F[c]	K_1	f[d]
2	Ethanol	284	*332*, 350	1	–	–
	Water/Ethanol/β-CD	282	334	1.6	310 ± 45	0.76
3	Ethanol	274	298	1	–	–
	Water/Ethanol/β-CD	276	306	2	390 ± 35	0.80
4	Ethanol	291	326	1	–	–
	Water/Ethanol/β-CD	278	328	3	330 ± 50	0.77

[a] NBD derivative concentration: 5×10^{-5} M; β-CD concentration: 0.01 M.
[b] λ_{ex}, λ_{em} = fluorescence excitation and emission wavelengths, respectively. Precision $\pm$ 1 nm.
[c] F = relative fluorescence intensity, calculated from the peak heights at the emission maximum, according to the ratio: F(medium)/F(ethanol).
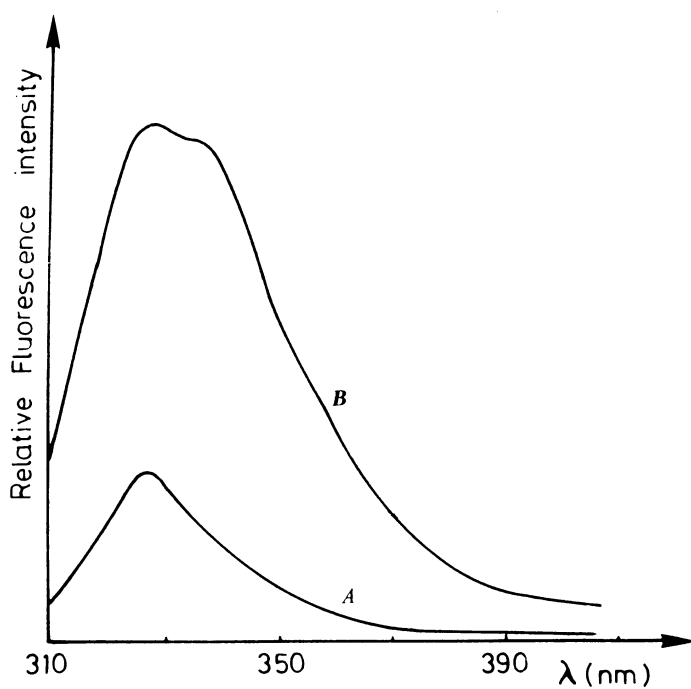[d] f = NBD molar complexed fraction in the presence of 0.01 M β-CD, calculated using Equation 1.

Figure 2. Fluorescence emission spectra of compound **4** (5×10^{-5} M) in ethanol (A), and in a 10^{-2} M β-CD 99 : 1 water–ethanol solution (B).

results from reduced mobility, a decrease in the molecular degrees of freedom, the creation of a favorable microenvironment and/or CD shielding against the solvent molecules and impurities, acting as potential quenchers and present in the bulk solution [1,2].

3.3. EFFECT OF INCREASING β-CD CONCENTRATION

The addition of increasing β-CD concentration (from [β-CD] = 0 to 0.01 M), to the NBD derivative (5 $\times$ 10^{-5} M) solutions significantly increases the complex fluorescence signal. Indeed, for the highest β-CD concentrations (0.01 M) the fluorescence intensity (F) is 1.6 to 3 times larger than in the absence of β-CD (Table II). The F vs. [β-CD] curves show a rapid increase in the region between 0 to 7 $\times$ 10^{-3} M, followed by a plateau region characterized by small increments of the intensity values until [β-CD] = 0.01 M. Assuming that the equilibrium of the complexation reaction does not change considerably during the NBD excited-state lifetime, and that no important conformational distortion as well as change of the NBD : β-CD ground-state interactions are occurring upon excitation, we can consider that the complex distribution is faithfully reflected by the fluorescence intensity increase. We have calculated the molar fraction (f) of the complexed NBD molecules in the plateau region, by using Equation (1) [38]:

$$f = 1 - \frac{1}{1 + K_1 \cdot [\text{HP–}\beta\text{-CD}]} \tag{1}$$

where K_1 is the formation constant of the inclusion complex. This parameter is calculated in the next section, using the correlation of relative fluorescence intensity with [β-CD]. As shown in Table II, the f values are higher than 0.75, indicating that a majority of NBD molecules are complexed by β-CD.

3.4. PROPERTIES OF THE NBD DERIVATIVES: β-CD INCLUSION COMPLEXES

The stoichiometry and formation constant of β-CD : NBD derivative inclusion complexes were determined as previously [6, 39, 40].

It was found that the NBD fluorescence intensity increased with increasing β-CD concentration, up to a constant value corresponding to a sufficient reagent excess. The relation between the fluorescence increment and the β-CD concentration can be expressed as follows [39]:

$$\frac{1}{F - F_0} = \frac{1}{(F_\infty - F_0) \cdot K_1 \cdot [\beta - CD]_0} + \frac{1}{F_\infty - F_0} \tag{2}$$

where F_0 and F_∞ denote the fluorescence intensities of NBD in the absence and in the presence of 0.01 M β-CD, and F is the observed fluorescence intensity at each β-CD concentration tested.
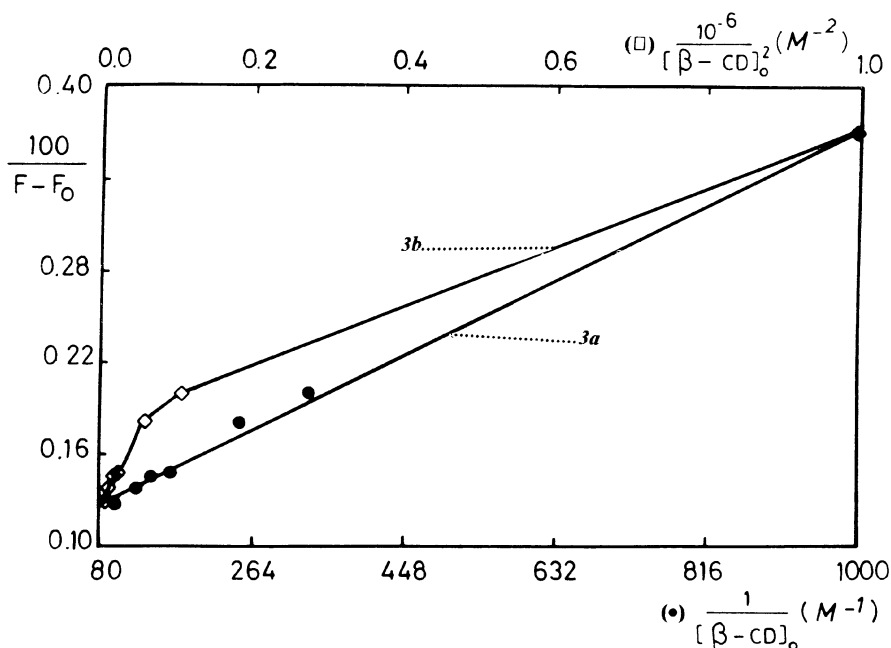
Figure 3. Double reciprocal plots for compound **4**. (a) A linear relationship is established when the data are plotted assuming a 1 : 1 NBD : β-CD stoichiometry (Equation 2). (b) A downward concave curvature is observed when the data are plotted assuming a 1 : 2 stoichiometry (Equation 3).

If the stoichiometry is 1 : 1, a linear plot should be established (Equation 2). If the complex stoichiometry was 2 : 1, a linear graph would be obtained when using Equation 3:

$$\frac{1}{F - F_0} = \frac{1}{(F_\infty - F_0) \cdot K_2 \cdot [\beta - CD]_0^2} + \frac{1}{F_\infty - F_0}. \tag{3}$$

As shown in Figure 3, a linear relationship is obtained when $1/F - F_0$ is plotted against $1/[\beta\text{-CD}]$, indicating that the stoichoimetry of the complex is 1 : 1 (curve 3a). In contrast, a downward, concave curvature is obtained when these data are fitted to a 2 : 1 complex (curve 3b). The linear plot can be used to obtain K_1, by simply dividing the intercept by the slope, but the Benesi–Hildebrand plots tend to place more emphasis on lower concentration values than on higher concentration values. Consequently, the slope is more sensitive to the ordinate value of the point having the smallest concentration. A better estimation is obtained by nonlinear regression analysis (NLR) [39, 40]. Rearranging the data, Equation 2 can be presented in the more familiar form [40], which gives a direct relationship between F and [β-CD],

$$F = F_0 + \frac{(F_\infty - F_0) \cdot K_1 \cdot [\beta - CD]_0}{1 + K_1 \cdot [\beta - CD]_0}. \tag{4}$$
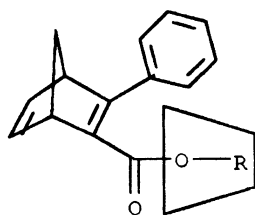
Scheme 2. Hypothetical structure of the inclusion complex.

Experimental data can be directly fitted by using this equation. The initial parameter estimates needed for NLR are obtained from the linear plots. The NLR analysis of the data has been performed by an iterative Marquardt-type process.
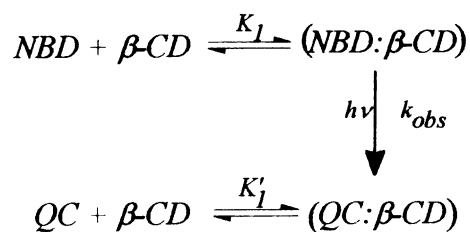
The theoretical model curves obtained by application of Equation 4, are in good agreement with the experimental data, confirming that the complex stoichiometry is 1 : 1. K_1 values are very close for the fluorescent NBD derivatives under study, ranging between 310 and 390 M^{-1} (Table II). This may indicate that the same molecular moiety is included in the β-CD cavity for all NBD derivatives.

Clearly, the geometry of inclusion of NBD derivatives in β-CD depends on the size of the various parts of these molecules. First, the dimensions of the NBD ring – predicted by the *ab initio* method [41], or by AM1 semi-empirical calculation – are approximately 2.4 Å in length (double bond interdistance), 2.1 Å in height (distance between the double bond plane and the bridged carbon), and 1.3 Å in width (unsubstituted double bond). Second, for the phenyl (or phenylester) groups, the distances between the *para* and *meta* aromatic carbons are 2.8 Å and 2.4 Å, respectively. These data indicate that any one of these sites (the NBD ring, the phenyl or the phenylester groups) is able to be included *axially* in the β-CD cavity, the internal diameter and the depth of which are about 6.2 Å and 7.9 Å, respectively [2]. However, because of the relatively great overall length of the NBD molecules (between 6.5 Å for compound **1**, and 14.9 Å for compound **4**, according to the AMI method), an *equatorial* inclusion is excluded, and axial inclusion should be only *partially* achieved.

The inclusion of the phenylester site in the β-CD cavity is supported by the enhancement of fluorescence intensity observed with increasing β-CD concentrations; this behaviour shows that this fluorophore group directly interacts with the host molecule (Scheme 2).

3.5. PHOTOISOMERIZATION STUDIES

Photoisomerisation was investigated by irradiating the NBD solutions at room temperature with the 284-nm filtered beam of a high-pressure mercury lamp (see Experimental Section). The photoreactivities were comparatively investigated in the three media under study. The photoreaction progress was monitored simultaneously by absorption and fluorescence techniques. Considering that complexation

$$NBD + \beta\text{-}CD \xrightleftharpoons{K_1} (NBD{:}\beta\text{-}CD)$$

$$h\nu \downarrow k_{obs}$$

$$QC + \beta\text{-}CD \xrightleftharpoons{K_1'} (QC{:}\beta\text{-}CD)$$

Scheme 3. NBD derivatives complexation–photoisomerization process.
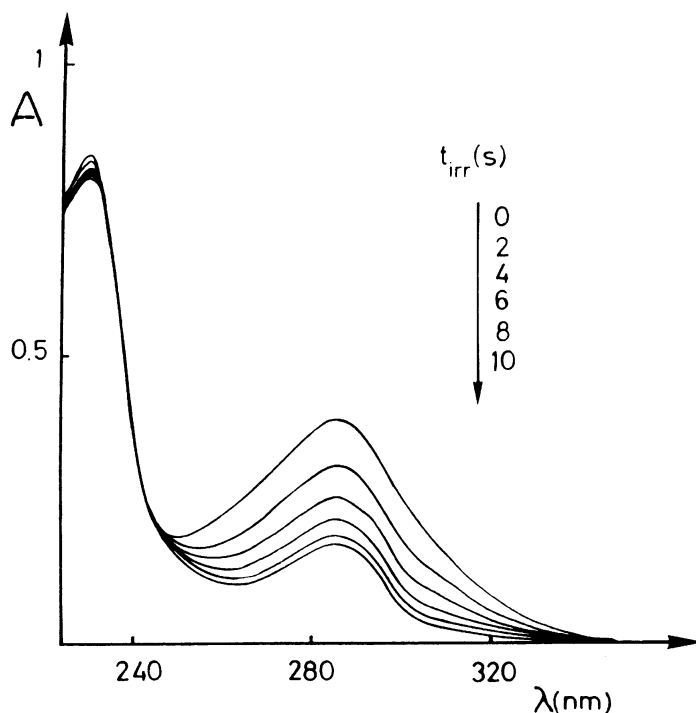

Figure 4. Evolution of the absorption spectra of derivative **4** (5×10^{-5} M) with irradiation time (t_{irr}) in WECD.

of NBD molecules takes place in the ground state (cf. Section 3.4), it can be expected that the formation of the host–guest complexes is a prior step to the photoisomerization reaction (Scheme 3).

The irradiation of NBDs in WECD is characterized by an important decrease of the long wavelength absorption bands located in the 270–300 nm region, and a relatively small increment of the 200–240-nm short wavelength band absorbance (Figure 4). The existence of an isosbestic point located at about 250 nm, shows that the photoisomerization reaction of the included NBDs proceeds without side reactions [28, 33, 34].
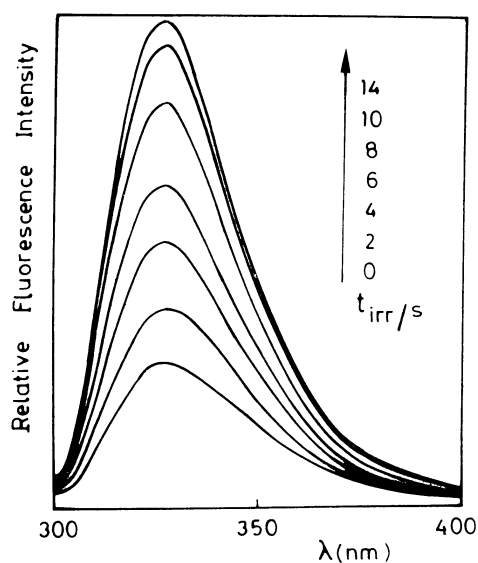
Figure 5. Evolution of the fluorescence emission spectra of derivative **4** (5×10^{-5} M) with irradiation time (t_{irr}) in WECD.

The evolution of fluorescence emission spectra with irradiation time is given in Figure 5, for the same NBD solutions. In contrast to the absorption spectral behaviour, the fluorescence intensity showed a marked increase with time. No significant change was observed in the position and shape of the fluorescence band during the photoreaction.

The spectral variations observed in WECD are similar to those found in ethanol. The phototransformation of the NBD moiety of compounds **1–4**, giving saturated QC, results in a significant decrease of the long wavelength absorption band intensity. This behaviour can be attributed to the disappearance of the conjugated π system, delocalized over the NBD double bond, monosubstituted phenyl and carbonyl groups.

Similar to our previous aromatic NBD photoisomerization studies in organic solvents [28], the fluorescence intensity enhancement occurring during photoisomerization in β-CD aqueous medium is probably due to the disappearance of the internal fluorescence quencher, i.e. the NBD ring. In contrast, an erratic kinetic behaviour was observed in the absence of β-CD (WE medium). This result demonstrates the role of specific β-CD interactions with NBD derivatives, confirming the formation of inclusion complexes. Indeed, in the configuration represented in Scheme 2, the complexed moiety of the NBD structure acts as a polar group favoring the solubility of the hydrophobic NBD derivatives and allowing the photoisomerization of NBD to take place in aqueous medium. Hydrosoluble NBD derivatives, functionalized with carbamoyl and carboxyl polar groups, have been also photoisomerized in alkaline aqueous solution [33], which supports our hypothesis on the

Table III. Medium effect on the observed photoisomerization rate constants $(k_{obs})^a$ of NBD derivatives.

	1		2		3		4	
	EtOH	WECD	EtOH	WECD	EtOH	WECD	EtOH	WECD
$k_{obs(A)}$	0.18	0.15	0.15	0.12	0.28	0.25	0.19	0.14
$k_{obs(F)}$	NF[b]	NF	0.12	0.10	0.27	0.15	0.19	0.12

[a] $k_{obs(A)}$ and $k_{obs(F)}$ are first-order rate constants (in s^{-1}) obtained spectrophotometrically (Equation 5) and spectrofluorimetrically (Equation 6), respectively, at 25°C for 5×10^{-5} M solutions. Relative standard error $\leq 10\%$.
[b] NF = compound not fluorescent.

complex structure. Moreover, the fact that the absorption and fluorescence spectra are not distorted after irradiation, suggests that the inclusion complexes are not destroyed during the photoreaction, but are still formed with the QC photoisomer derivatives (Scheme 3).

The spectral absorption and fluorescence kinetic data were treated, respectively, by the first-order Equations (5) and (6), based on the Guggenheim method [28, 35, 36]:

$$\ln(A - A') = k_{obs} t_{irr} + C \tag{5}$$

$$\ln(F' - F) = -k_{obs} t_{irr} + C' \tag{6}$$

where A, F and A', F' are the NBD solution absorbance (A) and fluorescence (F) intensities, measured at irradiation times t_{irr} and $t'_{irr} = t_{irr} + \theta$, respectively; θ is a constant time interval ($\theta = 2$ s); k_{obs} is the observed first-order rate constant, which depends on the incident light intensity: C and C' are the intercepts.

Linear plots were obtained when fitting the experimental data to Equations (5) and (6). Correlation coefficients are generally higher than 0.98 and relative standard errors do not exceed 10% (Table III). Therefore, it can be considered that the NBD photoisomerization reactions obey apparent first-order kinetics, in WECD as well as in EtOH. k_{obs} values measured spectrophotometrically were close to those evaluated by fluorescence (Table III).

Moreover, we must stress that the photoisomerization rate constants are of the same order of magnitude in both WECD and EtOH. Previously [28], we found a marked dependence of the NBDs photoisomerization rate constants on solvent polarity. Therefore, the kinetic results of this study indicate that the polarities of both media (WECD and EtOH) are probably similar.

4. Conclusion

We have shown that in aqueous media, hydrophobic NBD derivatives form with β-CD 1 : 1 stoichiometry complexes, resulting in a significant fluorescence enhance-

ment relative to free NBDs. Although the complex formation constants are relatively small, the complexed molar fraction of NBD molecules exceeds 0.75. The analysis of the complex molecular structure, based on AM1 geometric parameters and photophysical properties, suggests that inclusion is only partial and that the phenylester groups are probably encapsulated in the β-CD cavity.

From the photoisomerization kinetic studies, performed in various media, we can conclude that the formation of β-CD : NBD complexes takes place prior to photoisomerization and that it plays an essential role in the photoreactivity in aqueous medium.

References

1. K.H. Frömming and J. Szejtli: in J.E.D. Davies (ed.), *Topics in Inclusion Science: Cyclodextrins in Pharmacy*, Kluwer Academic Publishers, Dordrecht–Boston–London (1994), and references therein.
2. H.-J. Schneider: *Angew. Chem. Int. Ed. Engl.* **30**, 1417 (1991).
3. (a) I. Durán-Merás, A.Muñoz de la Peña, F. Salinas, and I. Rodriguez Cáceres: *Analyst* **119**, 1215 (1994). (b) Y.-B. Jiang: *Spectrochim. Acta* **51**, 275 (1995).
4. (a) N.J. Turro, G.S. Cox, and X. Li: *J. Photochem. Photobiol., A.: Chem.* **37**, 149 (1983). (b) S. Spcypinski and L. Cline Love: *J. Anal. Chem.* **56**, 331 (1984).
5. (a) A.Y. Will, J.M. Schuette-Parsons, R.A.Agbaria, and I.M.Warner: *Appl. Spectrosc.* **49**, 1762 (1995). (b) A.M. Stalcup and K.H. Gahm: *Anal. Chem.* **68**, 1369 (1996).
6. M. Maafi, B. Laassis, J.J. Aaron, M.C. Mahedero, A. Muñoz de la Peña, and F. Salinas: *J. Incl. Phenom.* **22**, 235 (1995).
7. T. Tamaki: *Chem. Lett.* **53** (1984).
8. (a) R. Chênevert and N.Voyer: *Tetrahedron Lett.* 5007 (1984). (b) R. Chênevert and R. Plante: *Can. J. Chem.* **6**, 1092 (1983).
9. L. Flamigni: *J. Chem. Soc., Faraday Trans.* **90**, 2331 (1994).
10. K. Kasatani, M. Ohashi, and H. Sato: *Carbohydr. Res.* **192**, 197 (1989).
11. M. Fukushima, T. Osa, and A. Ueno: *J. Chem. Soc., Chem. Commun.* 15 (1991).
12. M. Fukushima, T. Osa, and A. Ueno: *Chem. Lett.* 709 (1991).
13. F. Hirayama, T. Utsuki, and K. Uekama: *J. Chem. Soc., Chem. Commun.* 887 (1991).
14. F. Hamada, M. Fukushima, T. Osa, H. Ikeda, F. Toda, and A. Ueno: *Makromol. Chem., Rapid Commun.* **4**, 287 (1993).
15. T. Utsuki, K. Imamura, F. Hirayama, and K. Uekama: *Euro. J. Pharm. Sci.* **1**, 81 (1993).
16. R. S. Davison and J. Liu: *J. Photochem. Photobiol., A: Chem.* **71**, 121 (1993).
17. Y. Inoue, F. Dong, K. Yamamoto, L-H. Tong, H. Tsuneishi, T. Hakushi, and A. Tai: *J. Am. Chem. Soc.* **117**, 11033 (1995).
18. T. Ttsuki, F. Hirayama, and K. Uekama: *J. Chem. Soc. Perkin Trans. 2*, 109 (1993).
19. A. Ueno, M. Fukushima, and T. Osa: *J. Chem. Soc. Perkin Trans. 2*, 1067 (1990).
20. P. Bortolus and S. Monti: *J. Phys. Chem.* **91**, 5046 (1987).
21. A. Yabe, Y. Kawabata, H. Niino, M. Matsumoto, A. Ouchi, H. Takahashi, S. Tamura, W. Tagaki, H. Nakahara, and K. Fukuda: *Thin Solid Films* **160**, 33 (1988).
22. G.L. Duveneck, E.V. Sitzmann, K.B. Eisenthal, and N.J. Turro: *J. Phys. Chem.* **93**, 7166 (1989).
23. F. Hirayama, T. Utsuki, M. Yamasaki and K. Harata: *J. Pharm. Sci.* **81**, 817 (1992).
24. K. Hamasaki, A. Nakamura, K. Ueno, and F. Toda: *J. Incl. Phenom.* **13**, 349 (1992).
25. Y. Inoue, S. Kosaka, L. Matsumoto, H. Tsuneishi, T. Hakushi, A. Tai, K. Nakagawa, and L. H. Tong: *J. Photochem. Photobiol., A: Chem.* **71**, 61 (1993).
26. L.L. Costanzo, S. Giuffrida, S. Sortino, U. Chiacchio, and G. De Guidi: *J. Photochem. Photobiol., A: Chem.* **76**, 127 (1993).
27. (a) D.W. Rogers, F.C. MacLafferty, W. Fang, Q. Yang, and Y. Zhao: *Struct. Chem.* **3**, 53 (1992). (b) Q.H. Wu, B.W. Zhang, Y.F. Ming, and Y. Cao: *J. Photochem. Photobiol. A: Chem.* **61**, 53 (1991).

28. (a) M. Maafi, C. Lion, and J.J. Aaron: *New J. Chem.* **20**, 559 (1996). (b) M. Maafi, J.J. Aaron, and C. Lion: *Chem. Lett.* 1685 (1994).
29. (a) Z.I. Yoshida: *Heterocycles* 1 (1984). (b) K. Maruyama, H. Tamiaki, and S. Kawabata: *J. Chem. Soc. Perkin Trans. 2*, 543 (1986).
30. (a) E.E. Bonfantini and D.L. Officer: *J. Chem. Soc. Chem. Commun.* 1445 (1994). (b) K.-I. Hirao, A. Ando, T. Hamada, and O. Yonemitsu: *J. Chem. Soc. Chem. Commun.* 300 (1984). T. Iizawa, C. Hijikata, and T. Nishikubo: *Macromolecules* **25**, 21 (1992).
31. (a) S. Takamura, A. Kameyama, and T. Nishikubo: *Kobunshi Ronbunshi: Japanese Polym. Sci. Technol.* **52**, 684 (1995). (b) T. Iizawa, T. Sueyoshi, C. Hijikata, and T. Nishikubo: *J. Polym. Chem.* **32**, 3091 (1994). (c) M.E. Wright, G.D. Allred, R.B. Wardle, and L.F. Cannizo: *J. Org. Chem.* **58**, 4122 (1993).
32. M. Maafi, C. Lion, and J.J. Aaron: *Synthetic Metals.* **83**, 167 (1996).
33. (a) T. Nishikubo, H. Tamiaki, and T. Yanai: *Bull. Chem. Soc. Jpn.* **58**, 781 (1985). (b) K. Maruyama, H. Tamiaki, and S. Kawabata: *J. Org. Chem.* **50**, 4742 (1985).
34. T. Yumoto, K. Hayakawa, K. Kawase, H. Yamakita and H. Taoda: *Chem. Lett.* 1021 (1985).
35. M. Maafi, J.J. Aaron, and C. Lion: *J. Chim. Phys.* **94**, 477 (1997).
36. (a) L.J. Cline Love and M. Scrilec: *Anal. Chem.* **53**, 2103 (1981). (b) J.R. Bacon and J.N. Demas: *Anal. Chem.* **55**, 653 (1983).
37. (a) T. Kobayashi, Z-I. Yoshida, Y. Asako, S. Miki, and S Kato: *J. Am. Chem. Soc.* **109**, 5103 (1987). (b) R.C. Kookson, J. Dance, and M. Godfrey: *Tetrahedron* **24**, 1529 (1968).
38. L. Flamigni: *J. Phys. Chem.* **97**, 9566 (1993).
39. V.K. Smith, T.T. Ndou, A. Muñoz de la Peña, and I.M. Warner: *J. Incl. Phenom.* **10**, 363 (1991).
40. K.A. Connors: *Binding Constants, The Measurements of Molecular Complexity Stability*, John Wiley and Sons, New York (1987).
41. (a) K. Raghavachari, R.C. Haddon, and H.G. Roth: *J. Am. Chem. Soc.* **105**, 3110 (1983). (b) G. Knuchel, G. Grassi, B. Volgelsanger, and A. Bauder: *J. Am. Chem. Soc.* **115**, 10845 (1993).